

UC Berkeley

UC Berkeley Previously Published Works

Title

Soil moisture thresholds explain a shift from light-limited to water-limited sap velocity in the Central Amazon during the 2015–16 El Niño drought

Permalink

<https://escholarship.org/uc/item/5wg102pg>

Journal

Environmental Research Letters, 17(6)

ISSN

1748-9318

Authors

Meng, Lin
Chambers, Jeffrey
Koven, Charles
[et al.](#)

Publication Date

2022-06-01

DOI

10.1088/1748-9326/ac6f6d

Peer reviewed

1

1 **Soil moisture thresholds explain a shift from light-limited to water-limited sap**
2 **velocity in the Central Amazon during the 2015-16 El Niño drought**

3

4 **Lin Meng^{1*}, Jeffrey Chambers^{1,2}, Charles Koven¹, Gilberto Pastorello³, Bruno Gimenez^{4,5},**
5 **Kolby Jardine¹, Yao Tang¹, Nate McDowell⁶, Robinson Negron-Juarez¹, Marcos Longo¹,**
6 **Alessandro Araujo⁷, Javier Tomasella⁸, Clarissa Fontes⁹, Midhun Mohan^{1,2}, Niro Higuchi⁴**

8 ¹Climate and Ecosystem Sciences Division, Lawrence Berkeley National Laboratory, Berkeley,
9 CA 94720, USA

10 ²Department of Geography, University of California Berkeley, Berkeley, CA 94720, USA

11 ³Scientific Data Division, Lawrence Berkeley National Laboratory, Berkeley, CA, 94720, USA

12 ⁴National Institute of Amazonian Research (INPA), Manaus, Brazil

13 ⁵Center for Tropical Forest Science, Smithsonian Tropical Research Institute (STRI), Gamboa,
14 Republic of Panama

15 ⁶Earth Systems Science Division, Pacific Northwest National Laboratory, Richland, WA 99354,
16 USA

17 ⁷Embrapa Amazônia Oriental, Tv. Dr. Enéas Piheiro, s/n, Marco, CEP 66095-903, Caixa postal
18 48, Belém, Pará, Brazil

19 ⁸Centro Nacional de Monitoramento e Alertas de Desastres Naturais - CEMADEN, Parque
20 Tecnológico, Estrada Doutor Altino Bondensan, 500, São José dos Campos, SP, Brazil

21 ⁹Department of Integrative Biology, University of California, Berkeley, Berkeley, CA, 94720
22 USA

23 *Corresponding author. E-mail address: linmeng@lbl.gov

24 Abstract

25 Transpiration is often considered to be light- but not water-limited in humid tropical rainforests
26 due to abundant soil water, even during the dry seasons. The record-breaking 2015-16 El Niño
27 drought provided a unique opportunity to examine whether transpiration is constrained by water
28 under severe lack of rainfall. We measured sap velocity, soil water content, and meteorological
29 variables in an old-growth upland forest in the Central Amazon throughout the 2015-16 drought.
30 We found a rapid decline in sap velocity ($-38\% \pm 21\%$, mean \pm SD.) and in its temporal
31 variability (-88%) during the drought compared to the wet season. Such changes were
32 accompanied by a marked decline in soil moisture and an increase in temperature and vapor
33 pressure deficit. Sap velocity was largely limited by net radiation during the wet season;
34 however, it shifted to be primarily limited by soil moisture during the drought. The threshold in
35 which sap velocity became dominated by soil moisture was at $0.33 \text{ m}^3/\text{m}^3$ (around -150 kPa in
36 soil matric potential), below which sap velocity dropped steeply. Our study provides evidence
37 for a soil water threshold on transpiration in a moist tropical forest, suggesting a shift from light
38 limitation to water limitation under future climate characterized by increased temperature and an
39 increased frequency, intensity, duration and extent of extreme drought events.

40 Keywords: Drought, tropical forests, water cycle, soil moisture, evapotranspiration

41 **1. Introduction**

42 Transpiration in tropical forests plays a critical role in regulating the global water cycle and
43 climate (Chambers and Artaxo, 2017). Changes in forest transpiration have critical implications
44 for biosphere-atmosphere interactions at the local, regional, and global scales, influencing water
45 and carbon budgets as well as surface temperature (Fisher et al., 2008; Wright et al., 2017;
46 Grossiord et al., 2020; Li et al., 2016). The Sixth Assessment Report of the Intergovernmental
47 Panel on Climate Change (IPCC) showed robust projected increases in drought duration and
48 frequency with less rainfall and drying soil in the tropics (Arias, Paola, et al. 2021; Vogel et al.,
49 2020). A warmer and drier climate has already led to a series of impacts on tropical forest
50 ecosystems (Nepstad et al., 2002; McDowell et al., 2018). Transpiration underlies the
51 physiological responses of plants to drought, with warmer and drier conditions leading to
52 constraints on water uptake and subsequent downstream limitations on carbon uptake (Liu et al.,
53 2020). Understanding the physiological and ecological processes of tropical forests in response
54 to a more extreme environment is crucial to improve model predictions of the structure and
55 function of moist tropical forests under climate change (Ahlström et al., 2017; Gatti et al., 2014).

56 Transpiration is often limited by light availability in moist tropical forests (Roberts et al., 1993;
57 Shuttleworth, 1988; Von Randow et al., 2004; Meir et al., 2015; Nepstad et al., 2007; da Costa et
58 al., 2010) with moderation by drought (Grossiord et al. 2019). Deep soil water may remain
59 relatively abundant during dry seasons through rainfall recharge and via water redistribution
60 (e.g., by hydraulic lift; Lee et al., 2005; Oliveira et al., 2005). Thus soil moisture storage in the
61 rooting zone can be sufficient to maintain transpiration during the dry season (Juárez et al., 2007;
62 Wu et al., 2017; Yang et al., 2018). Soils have significant water storage capacity, and thus soil
63 moisture responses to drought can take several weeks to months after the dry periods—a
64 phenomenon called soil moisture memory (Da Rocha et al., 2009; Shuttleworth, 1988). Tropical
65 evergreen forests can progressively exploit water in the deeper layers of the soil during the dry
66 season when the shallow soil dries (Nepstad et al., 1994). Therefore, transpiration in moist
67 tropical forests is considered relatively insensitive to dry periods relative to the global average.

68 As the climate becomes warmer and drier, it is more likely that a threshold could be reached after
69 which soil moisture, instead of light availability, becomes a primary regulator of transpiration. In

70 2015–16, an unprecedented warm-phase El Niño drought occurred across the Amazon, providing
71 an opportunity to examine the physiological process of trees under future climate (Jiménez-
72 Muñoz et al., 2016). During this drought, record-breaking air temperature and extreme soil
73 moisture deficits occurred, accompanied by increased canopy turnover rate (Leitold et al., 2018),
74 a decline in sap velocity (Fontes et al., 2018; Gimenez et al., 2019), and increased influence of
75 vapor pressure deficit (VPD; the atmospheric evaporative demand; Grossiord et al. 2020). The
76 2015-16 drought was the warmest and driest drought since 1990 (Jiménez-Muñoz et al., 2016),
77 providing a rare opportunity to investigate how warmer droughts predicted to occur in the future
78 could impact transpiration in moist tropical forests.

79 In this study, we capitalized on the extreme 2015-16 drought through dry- and wet-season
80 measurements of transpiration and associated drivers in an old-growth upland forest in the
81 central Amazon to test for water limitations and identify if thresholds occurred. Our hypothesis is
82 that sap velocity during this event shifted from light-limitation to soil moisture limitations under
83 the particularly severe conditions experienced .

84 **2. Methods**

85 **2.1 Study site**

86 The study was conducted at the K34 tower (2.609 S, 60.209 W, 130 m) within the ZF-2 research
87 station in the Central Amazon, approximately 90 km north of the city of Manaus, Brazil. This
88 site has intermediate levels of rainfall within the Amazon biome and is typically light-limited
89 (Fontes et al., 2018). The K34 tower is 50-meter tall, located at the Reserva Biológica do
90 Cuieiras, is inside of extensive areas of undisturbed tropical forest (Araújo et al., 2002). The
91 topography of the region is characterized by a sequence of plateaus, slopes, and valleys (Ohta et
92 al., 1998), with the K34 tower located in a plateau area. The climate is characterized as tropical
93 rainforest (*Af*, according to Köppen climate classification) with the mean annual temperature
94 26.68 °C, annual rainfall of 2252 mm, and a moderate drier period between July and September
95 (Araújo et al., 2002). The vegetation is characterized by dense, old-growth, evergreen broadleaf
96 upland forest with a high diversity of tree species (Lima et al., 2007). Trees are on average 30 m
97 in height (Luizão et al., 2004). The most abundant botanical families in the ZF-2 research station
98 include *Lecythidaceae*, *Sapotaceae*, *Fabaceae*, *Chrysobalanaceae*, *Burseraceae*, *Annonaceae*,

99 *Moraceae*, and *Euphorbiaceae* (Vieira et al., 2004). The soil on the study site is dominated by
100 kaolinite, quartz, iron oxides and hydroxides, and Al, with high clay content but lacking P, Ca,
101 Mg, and K (Broedel et al., 2017; Luizão et al., 2004; Teixeira et al., 2014). In the top 30 cm of
102 the soil, clay contents constitute 65–75% and reach 80–90% into the 2 ~ 4 m soil layer (Negrón-
103 Juárez et al., 2020).

104 **2.2 Sap velocity measurements and processes**

105 We used heat pulse sap velocity sensors (SFM1, ICT international, Australia) to measure the sap
106 velocity of four representative individuals at the K34 tower from February, 2015 to December
107 31, 2017 (Table S1). These individuals are selected from the most abundant families and based
108 on the proximity of the crowns to the footprint of the K34 tower. Sensors were installed near
109 breast height on each tree following the protocols described in (Christianson et al., 2017). The
110 sensors measure sap velocity (cm h^{-1}) at 0.75 cm depth in the stem based on the heat ratio method
111 (Burgess et al., 2001; Steppe et al., 2010). The distance between needles is 5 mm, a factory
112 default setting recommended by the manufacturer (Burgess and Downey, 2014). The needle was
113 configured to emit a 20 Joule pulse of thermal energy every 15 min. The sap velocity Tool
114 version 1.4.1 (Phyto-IT) was used to calculate sap velocity for each tree using raw data measured
115 by sensors and biophysical characteristics (e.g., diameter and bark thickness). We conducted a
116 systematic removal of sap velocity observations associated with measurement failures and sensor
117 removals in the field. We assume that zero-flow conditions occur predawn and calibrate all
118 observations based on true zero flow conditions.

119 To quantify the dynamics of sap velocity and its variability, we first aggregated the raw sap
120 velocity data at every 15-minute timestep to a daily 90% quantile. The reason we used daily 90%
121 quantiles for aggregation is to robustly represent the extreme conditions during a day while
122 removing the influence of outliers or large fluctuations caused by short-term weather effects.
123 Then we calculated weekly sap velocity variability (i.e., the standard deviation of daily sap
124 velocity in each week) and normalized weekly sap velocity variability (i.e., sap velocity
125 variability divided by mean sap velocity in each week) from daily sap velocity. Normalized
126 weekly sap velocity variability (unit: percentage) describes the magnitude of sap velocity

127 fluctuation compared to the absolute value of sap velocity, and thus represents a critical indicator
128 of sap velocity in response to environmental changes.

129 **2.3 Environmental variables measurements**

130 Environmental variables including air temperature, relative humidity, VPD, net radiation, and
131 soil moisture were measured at the K34 tower. Air temperature and relative humidity were
132 measured using thermohygrometers (HC2S3, Campbell Scientific, Logan, UT, USA) at 50 m
133 (above the canopy) at the K34 tower data collection every minute and recorded as 30-minute
134 averages. VPD at 30-minute averages was calculated using air temperature and relative
135 humidity following the Clausius–Clapeyron equation. Net radiation (W/m^2) was calculated from
136 longwave in, longwave out, shortwave in, and shortwave out solar radiation, which were
137 collected with 5-min averages at 50 m using an NR-LITE sensor (Kipp & Zonen, Delft,
138 Netherlands). This dataset was provided by the Large-Scale Biosphere-Atmosphere Program
139 (LBA) project (Araújo et al., 2002).

140 Volumetric soil water content (SWC) was measured every 30 min at five soil depths: 5cm, 10cm,
141 20cm, 40cm, and 100 cm from January 2015 to July 2017. These measurements were performed
142 with a Water Content Reflectometer (CS655 Campbell Scientific, Logan, UT, USA) located
143 approximately 12 m from the K34 tower within the vegetation. Mean SWC of the top four layers
144 (i.e., 5cm, 10cm, 20cm, and 30cm) was used to examine environmental controls on sap velocity.

145 We also used daily precipitation and daily maximum temperature from 1990 to 2017 at the
146 Embrapa meteorological station at Adolfo Ducke Forest Reserve, located North of Manaus and
147 about 50 Km South of the K34 tower (available in the Embrapa InfoClima portal:

148 <https://www.cnpaf.embrapa.br/infoclima/>). These long time series daily data were then
149 aggregated to monthly sum precipitation and monthly mean maximum temperature and used to
150 compare climate conditions in 2015 to the long-term average.

151 **2.4 Soil water retention curve**

152 We used the following model that describes the soil water-release curve of van Genuchten
153 (1980):

$$\theta = \theta_r + \frac{\theta_s - \theta_r}{[1 + (\alpha|\psi|)^n]^m} \quad (1)$$

155 where θ is the volumetric soil water content (m^3/m^3), θ_s and θ_r are the saturated and residual
 156 water content (m^3/m^3), respectively, ψ is the absolute value of the matric potential (kPa). α (kPa⁻¹), n and m are parameters. m is taken to be $1-1/n$. Parameters of the van Genuchten equation
 157 were derived specifically for Manaus soil in Tomasella et al. (1996). We used the calibrated
 158 parameters θ_s , θ_r , α and n for 0.3m depth soil from Table 2 in Tomasella et al. (1996), and
 159 converted the soil moisture threshold to soil matric potential threshold.
 160

161 2.5 Statistical analysis

162 We first quantified the changes in the precipitation, VPD, air temperature, net radiation, SWC,
 163 and sap velocity before, during, and after the El Niño drought from 2015 to 2016. To do this, we
 164 aggregated precipitation from hourly to daily sum, and aggregated 30-minute observations to
 165 90% quantile daily observations for the rest of the variables for six two-week periods, i.e., wet
 166 seasons (March 1st to March 14th) in 2015 and 2016, early dry seasons (June 28th to July 12nd) in
 167 2015 and 2016, late dry season (August 19th to September 1st, 2015), and drought (September
 168 22nd to October 5th, 2015). Sap velocity and climate variables during these two-week periods
 169 represent the typical conditions for these periods. We also calculated the weekly sap velocity
 170 variability and the normalized weekly sap velocity variability to investigate sap velocity
 171 dynamics.

172 To examine the environmental controls on sap velocity, we used partial correlation analysis and
 173 multiple linear regression analysis to analyze the relationships between net radiation, SWC, and
 174 sap velocity for each individual tree during the six periods. Because net radiation and SWC are
 175 often correlated, the partial correlation analysis measures the degree of association between sap
 176 velocity and each variable with the confounding effects of other control variables excluded
 177 statistically at the same time (Beer et al., 2010). We also tested the interaction effect between
 178 SWC and net radiation on sap velocity for each of the six periods, respectively, in the multiple
 179 linear regression model. We only presented the model results with the interaction term when it
 180 was significant ($P < 0.05$). Data used in the multiple linear regression analysis and partial
 181 correlation analysis are daily 90% quantiles calculated from half-hour data.

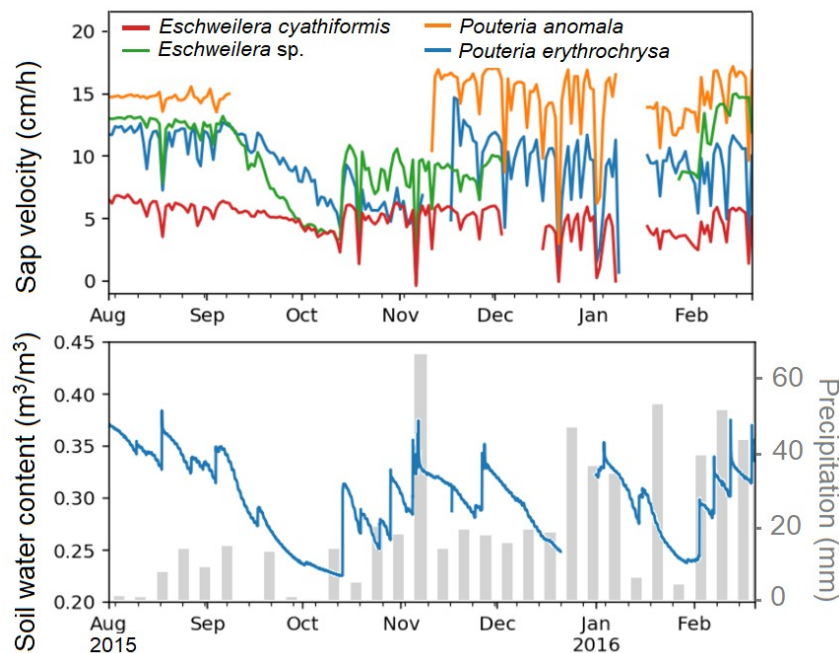
182 To identify the timing when sap velocity shifted from light-limited to soil moisture-limited and
183 the critical thresholds of soil moisture, we further conducted two moving-window partial
184 correlation analyses between net radiation, SWC, and sap velocity for each tree individual. First,
185 we conducted a partial correlation analysis for every 15-day period from August 1st, 2015 to
186 September 1st, 2016 with a 3-day moving step. Then we zoomed into the period from August
187 17th, 2015 to November 1st, 2015, and used a 10-day window period with a 1-day moving step,
188 focusing on identifying the accurate timing of water stress. Based on the partial correlation
189 coefficients between soil moisture and sap velocity (R_{swc}), we identified the date when soil
190 water stress started to occur as the first window period when R_{swc} of the following three
191 consecutive window periods are significant ($P < 0.05$). The statistical significance was
192 determined by a two-tailed Student's t-test.

193 **3. Results**

194 **3.1 Rapid transpiration collapse during the drought**

195 The 2015-16 El Niño drought was characterized by extreme climatic conditions, including low
196 rainfall and dry soil, and high radiation, temperature, and VPD (Figs.1-2). Continuous low
197 precipitation caused a substantial decrease in soil moisture, which happened simultaneously with
198 a $38\% \pm 21\%$ (mean \pm SD.) drop in sap velocity across all tree individuals, compared to the 2015
199 wet season (Figs. 1 and 3a). Precipitation showed a 96.8% decline from 115.91 mm during the
200 wet season (March 1st to March 14th, 2015) to 3.71 mm during the drought period (September
201 22nd to October 5th, 2015) and 90.4% decrease compared to the same period in the non-drought
202 year 2016 (38.8 mm) (Figs. 2a and S1a). Shallow (i.e., 5 cm beneath the surface) soil moisture
203 dropped markedly in response to the drought, from $0.40 \text{ m}^3/\text{m}^3$ in the 2015 early dry season to
204 $0.22 \text{ m}^3/\text{m}^3$ during the drought (i.e., a 45% decrease, Fig. S2). Deep soil moisture (100 cm
205 beneath the soil surface) was comparatively constant year-round, but still dropped $0.024 \text{ m}^3/\text{m}^3$
206 (6%) to $0.38 \text{ m}^3/\text{m}^3$ during the drought (Fig. S2). Compared to the same period in 2016, soil
207 moisture at 5cm and 100 cm decreased from $0.34 \text{ m}^3/\text{m}^3$ (by 35%) and $0.41 \text{ m}^3/\text{m}^3$ (by 7%),
208 respectively (Fig. S2). On an average, soil moisture of the top 30 cm decreased 31.6% from the
209 2015 early dry season ($0.38 \text{ m}^3/\text{m}^3$) to the drought ($0.26 \text{ m}^3/\text{m}^3$), and showed gradual recovery to
210 $0.37 \text{ m}^3/\text{m}^3$ in 2016 (Fig. 2b). At the same time, net radiation reached its maximum, i.e., 724 W/

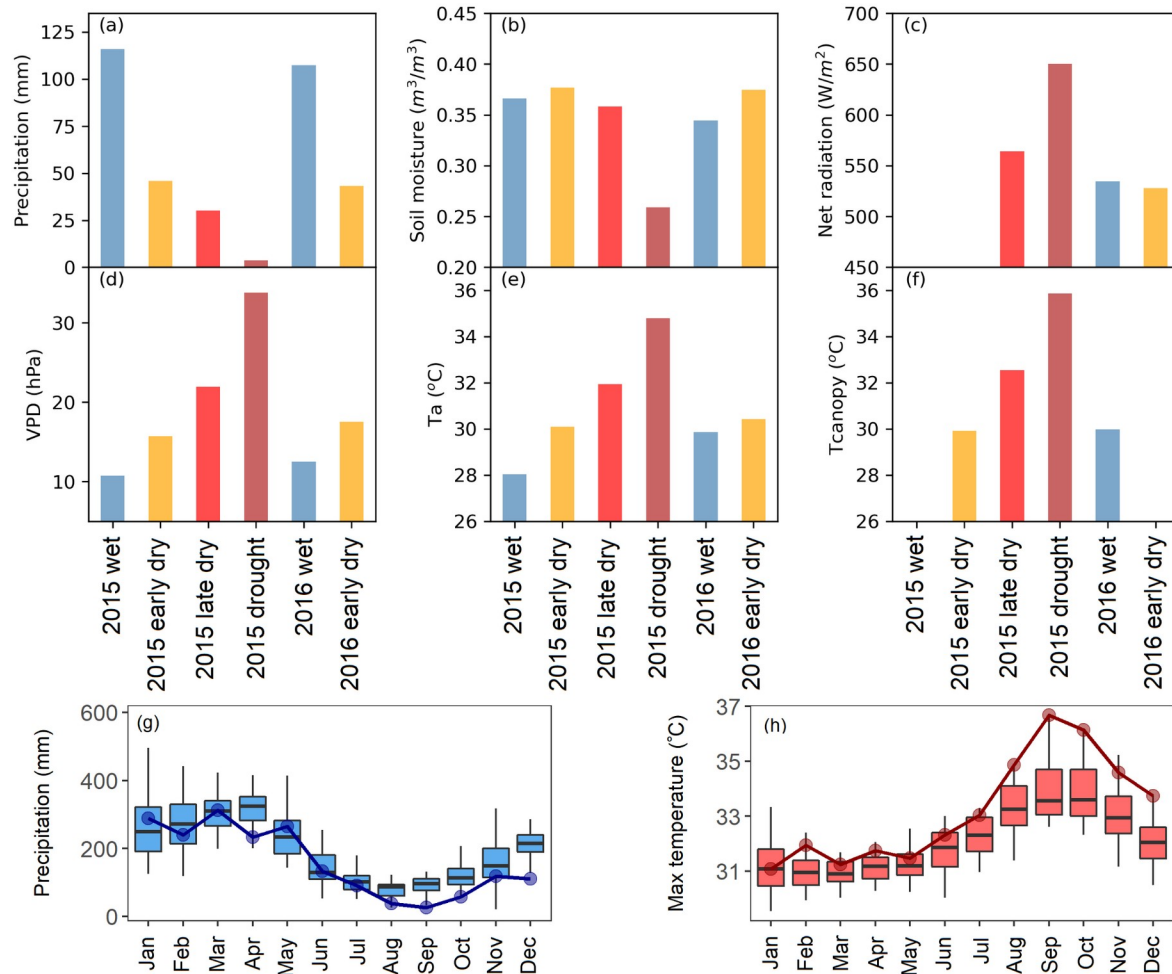
211 m², during the drought (Fig. S1). The transition from drought to the 2016 wet season was
 212 accompanied by a marked reduction in net radiation from 650 W/m² to 534 W/m² on average
 213 (Fig. 2c). VPD, air temperature, and canopy temperature showed similar changes, with gradual
 214 increases from wet to late dry seasons, reaching their maximum during the drought (33.8 hPa,
 215 34.8 °C and 35.9 °C, respectively), and dropped back to normal by the 2016 wet season (Fig. 2d-
 216 f). The rapid rise during the drought accounted for 215% and 6.8 °C increase in VPD and air
 217 temperature, respectively, compared to 2015 wet season (Fig. 2d-f). In early October, with
 218 increasing rainfall events, soil moisture started to increase, and sap velocity showed recovery as
 219 well (Fig. 1). Compared to long-term climate conditions, precipitation in September reached the
 220 minimum in 2015 (26.1 mm), while the mean precipitation in September was 93.7 mm during
 221 1990-2016 (Fig. 2g). More extremely, the maximum temperature in September reached its
 222 maximum (36.7 °C) in 2015, or 2.9°C above the 1990-2016 average (33.8 °C, Fig. 2h).



223

224 **Fig. 1 Dramatic drop in soil water content accompanied by a substantial decrease in sap**
 225 **velocity during the 2015 El Niño drought.** No data was collected for *Pouteria anomala*
 226 during September - November 2015. Weekly sum precipitation is shown as the gray bar.

227

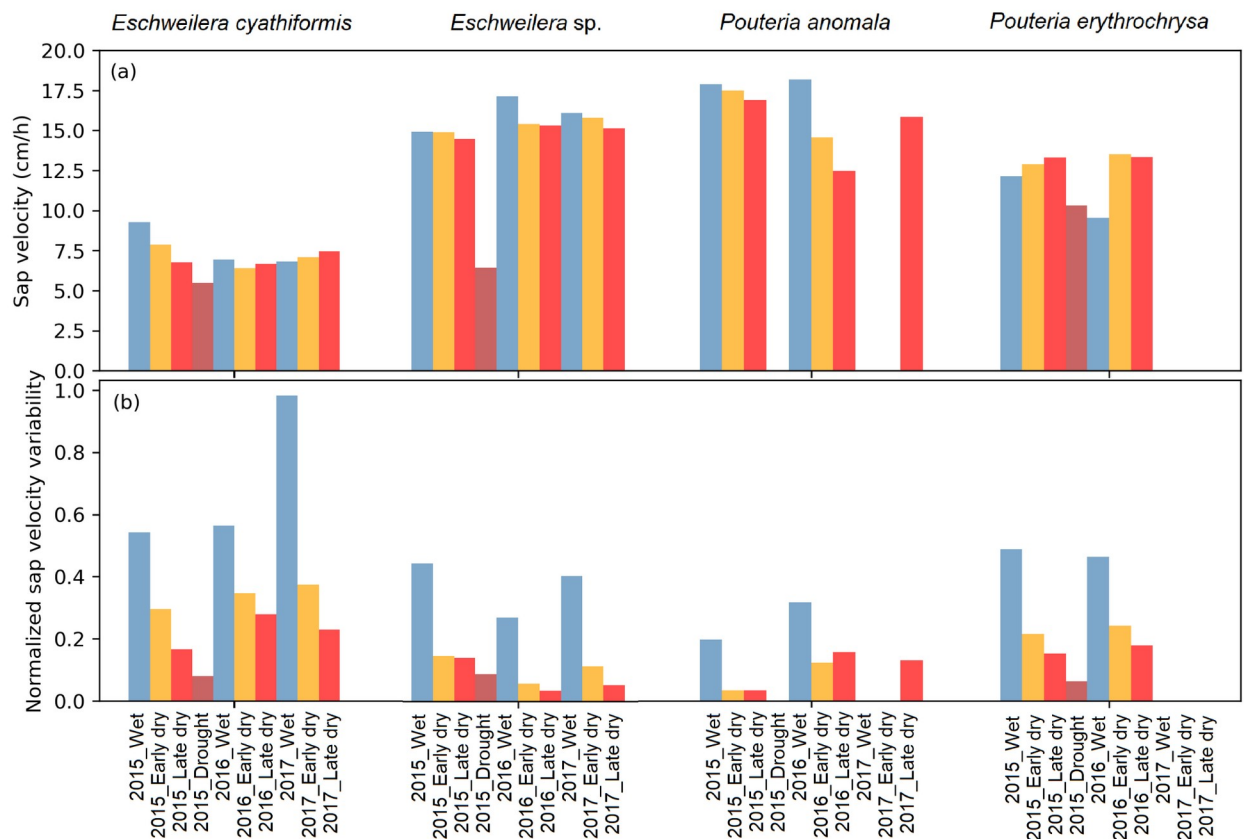


228

229 **Fig. 2 Extreme changes in environmental variables during the 2015 El Niño drought.** (a)-
 230 (f): Changes in environmental variables including during the wet season, early dry season, late
 231 dry season, and drought. No data was collected for net radiation during 2015 wet and early dry
 232 seasons, and for canopy temperature during 2015 wet season and 2016 early dry season. (g)-(h):
 233 Monthly precipitation (g) and maximum temperature (h) in 2015 (shown as line and points)
 234 compared with long-term mean during 1990-2016. The central line, lower and upper hinges in
 235 the box plots represent the median, 25th and 75th percentiles, respectively, of the precipitation or
 236 maximum temperature during 1990-2016.

237 Sap velocity of *Eschweilera cyathiformis*, *Eschweilera* sp., and *Pouteria erythrochrysa* declined
 238 rapidly by 41% (from 9.3 cm/h to 5.5 cm/h), 57% (from 14.9 cm/h to 6.4 cm/h), and 15% (from
 239 12.1 cm/h to 10.3 cm/h), respectively (No data was collected for *Pouteria anomala* during the

240 drought, Fig. 3a). Sap velocity recovered after a rainfall event in October, 2015 and kept the
 241 same magnitude during most of 2016-2017 as before drought (Fig. S3). The normalized sap
 242 velocity variability (i.e., the ratio of standard deviation of sap velocity and mean sap velocity)
 243 was the highest during wet seasons ($49\% \pm 5\%$, mean \pm SD.), gradually decreased during early
 244 and late dry season, reached its minimum during the drought ($7.6\% \pm 1.5\%$, mean \pm SD.), and
 245 recovered before the wet season in 2016 (Figs. 3b and S3c-d). For example, sap velocity
 246 variability of *Eschweilera cyathiformis*, *Eschweilera* sp., and *Pouteria erythrochrysa* decreased
 247 by 85.2% (from 54% to 8%), 79.5% (from 44% to 9%), and 87.8% (from 49% to 6%),
 248 respectively, from wet season to drought in 2015 (Fig. 3b).

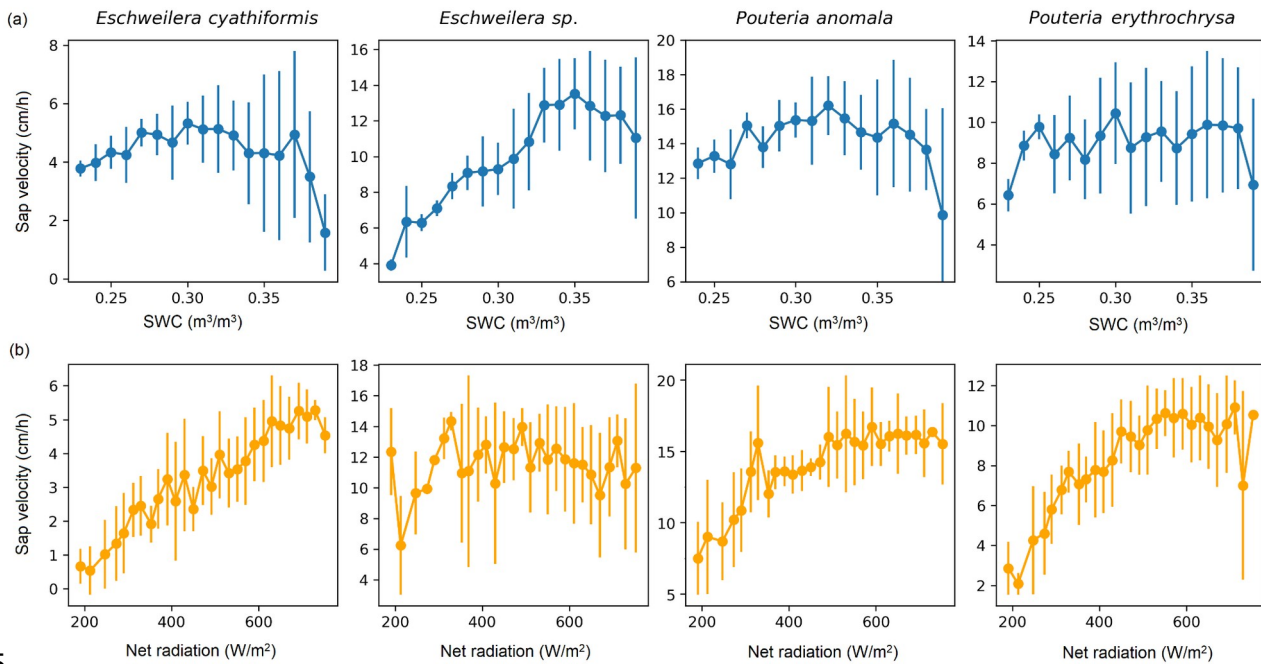


249

250 **Fig. 3 Sap velocity (a) and normalized sap velocity variability (b) during wet season, early**
 251 **dry season, late dry season, and drought from 2015 to 2017.** No data was collected for
 252 *Pouteria anomala* during the drought in 2015, and wet and early dry season in 2017.

253 3.2 Water and light limitations on sap velocity

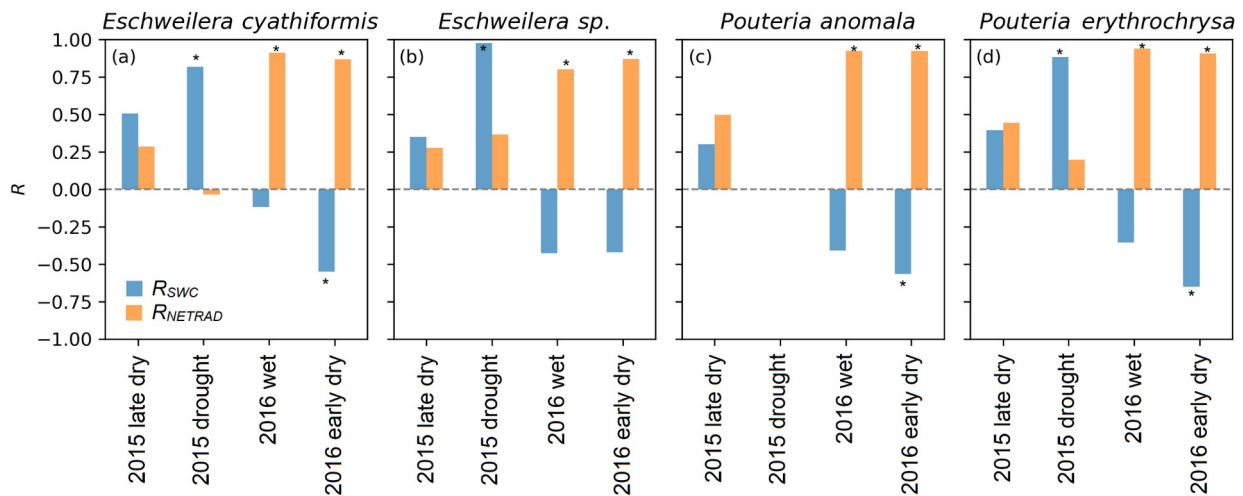
254 We found a strong positive correlation between sap velocity and net radiation during the entire
 255 study period, and a strong positive correlation between sap velocity and soil moisture only under
 256 low soil moisture (Fig. 4). Sap velocity declined with the decrease in soil moisture when soil
 257 moisture was below 0.3 m³/m³ (Fig. 4a), which occurred during the most severe drought period
 258 (Fig. S2). The variability of sap velocity in each soil moisture bin was small under low soil
 259 moisture (0.7 – 1.7 cm/h), but became large when soil moisture was above 0.3 m³/m³ (2.0 – 3.3
 260 cm/h, Fig. 4a). The relationship between net radiation and sap velocity is generally consistent
 261 across tree individuals, although with some minor variations (Fig. 4b). The response of sap
 262 velocity to the increase in net radiation is linear for *Eschweilera cyathiformis*, but nonlinear for
 263 *Pouteria anomala* and *Pouteria erythrochrysa*, reaching a plateau when net radiation approaches
 264 500 W/m². These results indicate a strong soil moisture control under dry conditions.



265 **Fig.4 Relationships between sap velocity and soil moisture (a) or net radiation (b).** Data
 266 used here are daily 90% quantile calculated from half-hour data. Data are binned at every 0.1 m³/
 267 m³ of soil moisture (a) and every 20 W/m² of net radiation (b). The dots and error bars for each
 268 m³ of soil moisture (a) and every 20 W/m² of net radiation (b). The dots and error bars for each
 269 bin show the mean and standard deviation for sap velocity, respectively.

270 We further found a clear shift from light to water limitation for all tree individuals using partial
 271 correlation analyses (Fig. 5). Sap velocity was largely limited by net radiation during wet and dry

272 seasons, but in contrast, only limited by soil moisture during the drought. The partial correlation
 273 coefficients between sap velocity and soil moisture (R_{swc}) showed gradual increases from late
 274 dry season to drought, and reached maximum values during the drought, i.e., 0.81, 0.98, and 0.88
 275 for *Eschweilera cyathiformis*, *Eschweilera sp.*, and *Pouteria erythrochrysa*, respectively (Fig. 5,
 276 $P < 0.05$). However, during the 2016 wet and early dry seasons, we found a dominant net
 277 radiation control on sap velocity. The partial correlation coefficients between sap velocity and net
 278 radiation (R_{NETRAD}) were higher than 0.87 for all tree individuals (Fig. 5, $P < 0.05$). It's worth
 279 noting the negative correlation between sap velocity and soil moisture during wet season (Fig. 5
 280 and at low radiation level in Fig. S4) is actually a light effect, i.e., decreased radiation in rainy
 281 days reduces sap velocity, which happens simultaneously when soil becomes moister. This
 282 finding directly supports our hypothesis that sap velocity was light-limited during the wet season
 283 and normal dry season but shifted to be soil moisture-limited during the drought. We also found
 284 predominant interaction effects between soil moisture and net radiation during wet and early dry
 285 seasons in 2016, but not during the late dry season and the drought in 2015, using the multiple
 286 linear regression models (Table S2, $P < 0.05$). This indicates that, with the increase in net
 287 radiation, sap velocity significantly increased under wet soil conditions but decreased under dry
 288 soil conditions (Fig. S4).



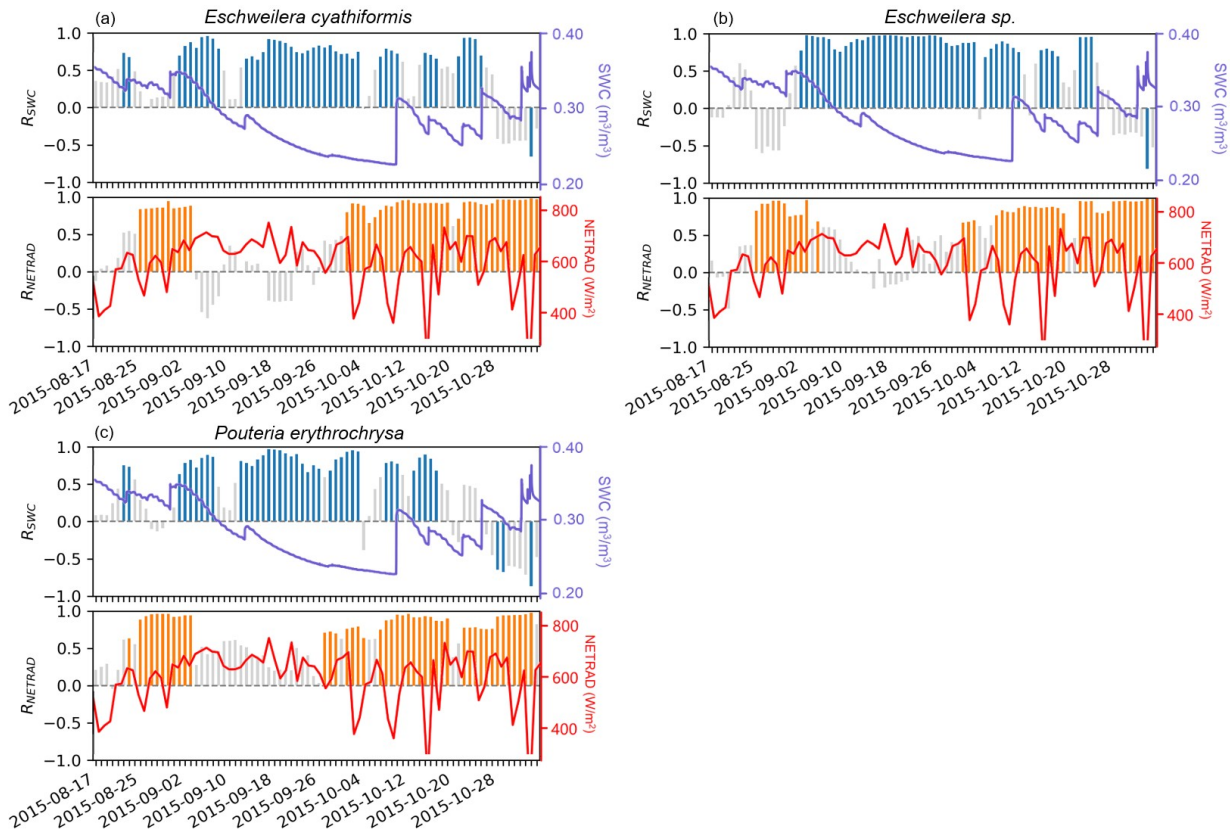
289

290 **Fig. 5 Partial correlation coefficients (R) between sap velocity and soil moisture or**
 291 **radiation during wet season, early dry season, late dry season, and drought. $P < 0.05$ (*).**

292 No sap velocity data were collected for *Pouteria anomala* during the 2015 drought.

293 3.3 Soil moisture threshold on sap velocity

294 Water stress started to occur on sap velocity across all individuals (i.e., sap velocity was
295 significantly positively correlated with soil moisture, $R_{swc} > 0$ and $P < 0.05$) in early September
296 2015, continued through the rest of September and first half of October, then became intermittent
297 and disappeared after several rainfall events (Figs.6 and S5). There was a profound light
298 limitation in August before the drought, and from October, 2015 to the whole of 2016, but not in
299 September, 2015 (Figs. 6 and S5). The period with strong water limitation was also the period
300 when soil moisture started to decrease (Fig. S2). There were several rainfall events in the middle
301 of the drought, during which soil moisture rapidly increased to some extent and the water
302 limitation disappeared for a short time (e.g., September 15th, 2015, Fig. 6). Based on the timing
303 of water stress, we identified the soil moisture threshold as $0.33 \text{ m}^3/\text{m}^3$ (mean of the top four
304 layers, Table 1). The corresponding soil matric potential threshold was -144 kPa on average
305 across individuals (Table 1 and Fig. S6), consistent with those found by Tomasella and Hodnett
306 (1996). Sap velocity of *Eschweilera* sp. was limited by soil moisture 2 days later than
307 *Eschweilera cyathiformis* and *Pouteria erythrochrysa* (i.e., Sep. 3 -Sep. 12), when soil moisture
308 and matric potential were $0.327 \text{ m}^3/\text{m}^3$ and -185 kPa, respectively (Table 1).



309

310 **Fig. 6 Moving window of partial correlation coefficient (R) between sap velocity, soil**
 311 **moisture, and net radiation.** The moving step and window length are 1 day and 10 days,
 312 respectively. The blue and orange bars represent the significant partial correlation coefficient
 313 between sap velocity and soil moisture (R_{SWC}) and between sap velocity and net radiation
 314 (R_{NETRAD}), respectively ($P < 0.05$). The gray bars represent non-significant coefficients ($P > 0.05$).

315 **Table 1 Identified periods and thresholds of soil moisture on sap velocity.** The water
 316 limitation period is the first window period when R_{SWC} of the following three continuous window
 317 periods are significant $P < 0.05$ from Fig.6. Mean soil water content of the top four layers (i.e.,
 318 5cm, 10cm, 20cm, and 30cm) and the corresponding soil matric potential (calculated based on
 319 equation (1), Fig. S6) are shown for each tree.

Species	Water stress period	Soil water content (m^3/m^3)	Soil matric potential (-kPa)
<i>Eschweilera cyathiformis</i>	Sep. 1 -Sep. 10	0.332	123
<i>Eschweilera sp.</i>	Sep. 3 -Sep. 12	0.327	185

<i>Pouteria erythrochrysa</i>	Sep. 1 -Sep. 10	0.332	123
Mean		0.330	144

320 4. Discussion

321 This study showed a shift from light-limited to water-limited transpiration of humid rainforests
322 and a soil moisture threshold that determines when the shift occurs even in regions where
323 water is often abundant. Previous studies have suggested that tropical evergreen forests in the
324 Central Amazon are not limited by water (Nepstad et al., 1994; Yang et al., 2018). However,
325 during the 2015-16 El Niño drought, photosynthesis decreased due to stomatal closure (Santos et
326 al., 2018), and sap velocity declined because of widespread embolism in the xylem (Fontes et al.,
327 2018). When soil becomes very dry and plant roots cannot absorb enough water to satisfy
328 transpiration from its leaves, the xylem water tension could raise above a threshold, causing
329 rupture of the water column and vessels to become embolized (Oliveira et al., 2021). Embolism
330 reduces the water transport capacity, further increasing xylem water tension and generating more
331 embolism, causing the leaf to lose turgor, the stomata to close, and consequently the decrease in
332 transpiration (Garcia et al., 2021). Taller trees exhibited lower embolism resistance and greater
333 stomatal sensitivity, suggesting a conservative hydraulic strategy of trees to endure drought,
334 with trade-offs between investing in xylem to reduce hydraulic vulnerability and actively
335 regulating stomatal responses to protect against low water potentials (Garcia et al., 2021).

336 Considering the broad environmental variation across Amazonia, our finding may not apply
337 to other regions in the Amazon. Steep gradients of soil fertility and precipitation across the
338 Amazon basin give rise to considerable variation in floristics, forest structure, and functional
339 traits. Diverse topography (e.g., plateaus, slopes and valleys) at a local scale also causes
340 variation in actual water available to forests, shaping the plant response to drought (Harper et al.,
341 2010; Hutyra et al., 2007). For example, during the same 2015-16 El Niño drought, no water
342 stress was found in the lowland eastern Amazon (Brum et al., 2018). The presence of deeper
343 roots systems (Nepstad et al., 1994) combined with hydraulic redistribution (Oliveira et al.,
344 2005) in the Eastern Amazon are possible mechanisms that may contribute to a higher tolerance
345 of these tropical forests to drought (Esteban et al., 2021). In addition, unlike the high clay content
346 soils in the Central Amazon, Eastern Amazon has high sand content soils (Negrón-Juárez et al.,

347 2020). Plants in the Eastern Amazon have direct access to groundwater, while plants in the
348 Central Amazon plateaus are more dependent on rainfall and thus experience higher water
349 deficits (Cosme et al., 2017; Fan et al., 2017; Fontes et al., 2020). As a result, plateau species
350 tended to have hydraulic safety traits while valley species tended to have hydraulic efficiency
351 traits, and the latter are relatively unaffected during droughts (Barros et al., 2019; Cosme et al.,
352 2017; Tomasella et al. 2008). In addition, a previous study of Broedel et al. (2017) in the same
353 Manaus site as the current study found no evidence of water stress during the less intense
354 drought of 2005. It is likely that the water stress found in this study is restricted to the most
355 intense droughts and El Niño droughts.

356 The soil moisture threshold observed in this study has critical implications for tropical
357 ecosystems under future climate change. Humid rainforests in the Central Amazon is generally
358 limited by light but not by water, and they may not depend on drought-resistance
359 hydraulic strategies during the drought, due to typically having sufficient water to satisfy growth
360 and survival requirements (Juárez et al., 2007; Yang et al., 2018). However, extreme climate
361 conditions with declines in precipitation and increases in temperatures are projected in the
362 future in the Amazon, likely reducing plant available water and placing tropical rainforests at
363 risk (Fung et al., 2005). If important ecological thresholds are passed, the resulting changes in
364 ecosystem service and function could be rapid and potentially substantial (Meir et al., 2015),
365 such as high mortality (Meir et al., 2015). The specific threshold of soil moisture in other
366 Amazon regions need to be identified for a comprehensive understanding of soil water stress
367 under extreme climate conditions (Longo et al., 2018). Such soil moisture thresholds also
368 provide a crucial benchmark to test and improve model simulations of future land-atmosphere
369 feedbacks under climate change, which are currently inadequate due to moisture deficit
370 insensitivity (Galbraith et al., 2010; Powell et al., 2013). It is possible that the physiological
371 effects of elevated CO₂ may ameliorate these water stresses in the future (Swann et al., 2016),
372 however at scales greater than the leaf it is not clear whether these effects are sufficient to allow
373 plants to sustain functioning when soils are dry, and further, whether feedbacks to precipitation
374 in response to CO₂-driven physiological changes may actually make the Amazon even more
375 vulnerable to drought (Kooperman et al., 2018). These thus represent further uncertainties in
376 projecting Amazon responses to future drought.

377 Collecting field data on soil moisture profiles and sap velocity across species at spatially diverse
378 sites is an essential step to identify soil moisture thresholds in other tropical regions to advance
379 mechanistic understanding and to improve predictive land surface models of ecosystem function.
380 However, realistic and sufficient sampling to obtain plot-level estimates in diverse plant
381 communities is very challenging (Baraloto et al., 2010). The measurements of sap velocity in this
382 study provide the only data available that cover the entire drought period, thus allow us to reveal
383 the shift from light to water limitation. However, it's worth noting that these valuable and high-
384 quality field data have very limited sample size due to logistical constraints. The findings
385 hold true for the studied individual tree species sampled in this study, but other species or
386 other sizes of trees in the studied rainforest might respond differently during the same magnitude
387 of drought. Further field measurements that are based on more complete sampling strategies,
388 such as sufficient sampling intensity, full representation of each species, and key functional traits,
389 are needed to fully understand the variation across regions and species. In addition, this study
390 consists of the first step to understand water constrain on humid rainforest, and further
391 investigation with more species, more sizes, and soil evaporation is needed to calculate stand
392 evapotranspiration and estimate the effect of drought on water relations at a stand-level.

393 **5. Conclusion**

394 This study provides robust evidence on water stress in the humid rainforest in Central
395 Amazon by showing an integration of multiple lines of observations including soil (soil
396 moisture), plants (sap velocity), and atmosphere (precipitation, net radiation, VPD, and
397 temperature) revealing plant physiological response during the progression of a severe
398 drought. Sap velocity was largely limited by net radiation during wet and dry seasons, as is
399 expected for the Central Amazon, but shifted to be limited only by soil moisture during the
400 drought. The soil moisture threshold in the Central Amazon was identified, implying that even
401 tropical rainforests in water abundant regions can be rapidly pushed out of the hydraulic safety
402 zone and limited by soil water deficits during extreme droughts. The ability of tropical forests in
403 the Amazon to survive in the future largely depends on their acclimation and adaptation to drier
404 conditions.

405 **Acknowledgement**

406 This work is supported by the Next Generation Ecosystem Experiments-Tropics (NGEE-
407 Tropics), as part of DOE's Terrestrial Ecosystem Science Program – Contract No. DE-AC02-
408 05CH11231. We would like to thank the Large Scale Biosphere-Atmosphere Program (LBA),
409 coordinated by the National Institute for Amazon Researches (INPA), for the use and availability
410 of data, for logistical support and infrastructure during field activities.

411 **Data availability statement**

412 The data that support the findings of this study are openly available at
413 <https://ngt-data.lbl.gov/doi/NGT0100/>. All data that support the findings of this study are
414 included within the article (and any supplementary files).

415 **References**

- 416 Ahlström, A. et al., 2017. Hydrologic resilience and Amazon productivity. *Nature*
417 *communications*, 8(1): 1-9.
- 418 Araújo, A. et al., 2002. Comparative measurements of carbon dioxide fluxes from two nearby
419 towers in a central Amazonian rainforest: The Manaus LBA site. *Journal of Geophysical*
420 *Research: Atmospheres*, 107(D20): LBA 58-1-LBA 58-20.
- 421 Arias, Paola, et al, 2021. *Climate Change 2021: The Physical Science Basis. Contribution of*
422 *Working Group14 I to the Sixth Assessment Report of the Intergovernmental Panel on*
423 *Climate Change; Technical Summary.*
- 424 Avissar, R., Silva Dias, P.L., Silva Dias, M.A. and Nobre, C., 2002. The large-scale biosphere-
425 atmosphere experiment in Amazonia (LBA): Insights and future research needs. *Journal*
426 *of Geophysical Research: Atmospheres*, 107(D20): LBA 54-1-LBA 54-6.
- 427 Baraloto, Christopher, et al, 2010. Functional trait variation and sampling strategies in species-
428 rich plant communities. *Functional Ecology* 24.1: 208-216.
- 429 Barros, F.d.V. et al., 2019. Hydraulic traits explain differential responses of Amazonian forests to
430 the 2015 El Niño-induced drought. *New Phytologist*, 223(3): 1253-1266.
- 431 Beer, C. et al., 2010. Terrestrial gross carbon dioxide uptake: global distribution and covariation
432 with climate. *Science*, 329(5993): 834-838.
- 433 Bencze, Szilvia, et al. 2014. Physiological response of wheat varieties to elevated atmospheric
434 CO₂ and low water supply levels. *Photosynthetica* 52.1: 71-82.
- 435 Broedel, E., Tomasella, J., Cândido, L.A. and Von Randow, C., 2017. Deep soil water dynamics
436 in an undisturbed primary forest in central Amazonia: Differences between normal years
437 and the 2005 drought. *Hydrological Processes*, 31(9): 1749-1759.
- 438 Brum, M. et al., 2018. ENSO effects on the transpiration of eastern Amazon trees. *Philosophical*
439 *Transactions of the Royal Society B: Biological Sciences*, 373(1760): 20180085.
- 440 Burgess, S. and Downey, A., 2014. SFM1 sap flow meter manual. ICT International Pty Ltd.:
441 Armidale, NSW, Australia.
- 442 Burgess, S.S. et al., 2001. An improved heat pulse method to measure low and reverse rates of
443 sap flow in woody plants. *Tree physiology*, 21(9): 589-598.
- 444 Chambers, J.Q. and Artaxo, P., 2017. Deforestation size influences rainfall. *Nature Climate*
445 *Change*, 7(3): 175-176.
- 446 Christianson, D.S. et al., 2017. A metadata reporting framework (FRAMES) for synthesis of
447 ecohydrological observations. *Ecological Informatics*, 42: 148-158.
- 448 Cosme, L.H., Schietti, J., Costa, F.R. and Oliveira, R.S., 2017. The importance of hydraulic

- 449 architecture to the distribution patterns of trees in a central Amazonian forest. *New*
450 *Phytologist*, 215(1): 113-125.
- 451 da Costa, A.C.L. et al., 2010. Effect of 7 yr of experimental drought on vegetation dynamics and
452 biomass storage of an eastern Amazonian rainforest. *New Phytologist*, 187(3): 579-591.
- 453 Da Rocha, H.R. et al., 2004. Seasonality of water and heat fluxes over a tropical forest in eastern
454 Amazonia. *Ecological applications*, 14(sp4): 22-32.
- 455 Da Rocha, H.R., Manzi, A.O. and Shuttleworth, J., 2009. Evapotranspiration. *Amazonia and*
456 *Global Change*, 186: 261-272.
- 457 Dickinson, R.E. and Henderson-Sellers, A., 1988. Modelling tropical deforestation: A study of
458 GCM land-surface parametrizations. *Quarterly Journal of the Royal Meteorological*
459 *Society*, 114(480): 439-462.
- 460 Doughty, C.E. et al., 2015. Drought impact on forest carbon dynamics and fluxes in Amazonia.
461 *Nature*, 519(7541): 78-82.
- 462 Esteban, E.J., Castilho, C.V., Melgaço, K.L. and Costa, F.R., 2021. The other side of droughts:
463 wet extremes and topography as buffers of negative drought effects in an Amazonian
464 forest. *New Phytologist*, 229(4): 1995-2006.
- 465 Fan, Y., Miguez-Macho, G., Jobbágy, E.G., Jackson, R.B. and Otero-Casal, C., 2017.
466 Hydrologic regulation of plant rooting depth. *Proceedings of the National Academy of*
467 *Sciences*, 114(40): 10572-10577.
- 468 Fisher, J.B., Tu, K.P. and Baldocchi, D.D., 2008. Global estimates of the land-atmosphere water
469 flux based on monthly AVHRR and ISLSCP-II data, validated at 16 FLUXNET sites.
470 *Remote Sensing of Environment*, 112(3): 901-919.
- 471 Fontes, C.G. et al., 2018. Dry and hot: the hydraulic consequences of a climate change-type
472 drought for Amazonian trees. *Philosophical Transactions of the Royal Society B:*
473 *Biological Sciences*, 373(1760): 20180209.
- 474 Fontes, C.G. et al., 2020. Convergent evolution of tree hydraulic traits in Amazonian habitats:
475 implications for community assemblage and vulnerability to drought. *New Phytologist*,
476 228(1): 106-120.
- 477 Fung, I.Y., Doney, S.C., Lindsay, K. and John, J., 2005. Evolution of carbon sinks in a changing
478 climate. *Proceedings of the National Academy of Sciences*, 102(32): 11201-11206.
- 479 Galbraith, D. et al., 2010. Multiple mechanisms of Amazonian forest biomass losses in three
480 dynamic global vegetation models under climate change. *New Phytologist*, 187(3): 647-
481 665.
- 482 Garcia, M.N. et al., 2021. Importance of hydraulic strategy trade-offs in structuring response of
483 canopy trees to extreme drought in central Amazon. *Oecologia*: 1-12.

- 484 Gatti, L. et al., 2014. Drought sensitivity of Amazonian carbon balance revealed by atmospheric
485 measurements. *Nature*, 506(7486): 76-80.
- 486 Gimenez, B.O. et al., 2019. Species-specific shifts in diurnal sap velocity dynamics and
487 hysteretic behavior of ecophysiological variables during the 2015–2016 el niño event in
488 the amazon forest. *Frontiers in plant science*, 10: 830.
- 489 Grossiord, C. et al., 2020. Plant responses to rising vapor pressure deficit. *New Phytologist*,
490 226(6): 1550-1566.
- 491 Grossiord, C. et al., 2019. Precipitation mediates sap flux sensitivity to evaporative demand in
492 the neotropics. *Oecologia*, 191(3): 519-530.
- 493 Guan, K. et al., 2015. Photosynthetic seasonality of global tropical forests constrained by
494 hydroclimate. *Nature Geoscience*, 8(4): 284-289.
- 495 Harper, A.B. et al., 2010. Role of deep soil moisture in modulating climate in the Amazon
496 rainforest. *Geophysical Research Letters*, Marked differences between van Genuchten
497 soil water-retention parameters for temperate and tropical soils: a new water-retention
498 pedo-transfer functions developed for tropical soils. *Geoderma*7(5).
- 499 Hodnett, M. and Tomasella, J., 2002. Marked differences between van Genuchten soil water-
500 retention parameters for temperate and tropical soils: a new water-retention pedo-transfer
501 functions developed for tropical soils. *Geoderma*, 108(3-4): 155-180.
- 502 Hutyra, L.R. et al., 2005. Climatic variability and vegetation vulnerability in Amazonia.
503 *Geophysical Research Letters*, 32(24).
- 504 Hutyra, L.R. et al., 2007. Seasonal controls on the exchange of carbon and water in an
505 Amazonian rain forest. *Journal of Geophysical Research: Biogeosciences*, 112(G3).
- 506 Jiménez-Muñoz, J.C. et al., 2016. Record-breaking warming and extreme drought in the Amazon
507 rainforest during the course of El Niño 2015–2016. *Scientific reports*, 6(1): 1-7.
- 508 Juárez, R.I.N., Hodnett, M.G., Fu, R., Goulden, M.L. and Von Randow, C., 2007. Control of dry
509 season evapotranspiration over the Amazonian forest as inferred from observations at a
510 southern Amazon forest site. *Journal of Climate*, 20(12): 2827-2839.
- 511 Koster, R.D. and Suarez, M.J., 2001. Soil moisture memory in climate models. *Journal of*
512 *hydrometeorology*, 2(6): 558-570.
- 513 Kooperman, Gabriel J., et al. 2018. Forest response to rising CO2 drives zonally asymmetric
514 rainfall change over tropical land. *Nature Climate Change* 8.5: 434-440.
- 515 Lee, J.-E., Oliveira, R.S., Dawson, T.E. and Fung, I., 2005. Root functioning modifies seasonal
516 climate. *Proceedings of the National Academy of Sciences*, 102(49): 17576-17581.
- 517 Leitold, V. et al., 2018. El Niño drought increased canopy turnover in Amazon forests. *New*
518 *Phytologist*, 219(3): 959-971.

- 519 Lima, A.J.N., Teixeira, L.M., Carneiro, V.M.C., Santos, J.d. and Higuchi, N., 2007. Biomass
520 stock and structural analysis of a secondary forest in Manaus (AM) region, ten years after
521 clear cutting followed by fire. *Acta amazonica*, 37(1): 49-53.
- 522 Li, H., Wang, A., Yuan, F., Guan, D., Jin, C., Wu, J., & Zhao, T. (2016). Evapotranspiration
523 dynamics over a temperate meadow ecosystem in eastern Inner Mongolia, China.
524 *Environmental Earth Sciences*, 75(11), 1-11.
- 525 Liu, Y., Kumar, M., Katul, G.G., Feng, X. and Konings, A.G., 2020. Plant hydraulics
526 accentuates the effect of atmospheric moisture stress on transpiration. *Nature Climate*
527 *Change*: 1-5.
- 528 Longo, M. et al., 2018. Ecosystem heterogeneity and diversity mitigate Amazon forest resilience
529 to frequent extreme droughts. *New Phytologist*, 219(3): 914-931.
- 530 Luizão, R.C. et al., 2004. Variation of carbon and nitrogen cycling processes along a topographic
531 gradient in a central Amazonian forest. *Global Change Biology*, 10(5): 592-600.
- 532 Malhi, Y. et al., 2002. Energy and water dynamics of a central Amazonian rain forest. *Journal of*
533 *Geophysical Research: Atmospheres*, 107(D20): LBA 45-1-LBA 45-17.
- 534 McDowell, N. et al., 2018. Drivers and mechanisms of tree mortality in moist tropical forests.
535 *New Phytologist*, 219(3): 851-869.
- 536 Meinzer, F.C., James, S.A. and Goldstein, G., 2004. Dynamics of transpiration, sap flow and use
537 of stored water in tropical forest canopy trees. *Tree physiology*, 24(8): 901-909.
- 538 Meir, P. et al., 2015. Threshold responses to soil moisture deficit by trees and soil in tropical rain
539 forests: insights from field experiments. *BioScience*, 65(9): 882-892.
- 540 Moreira, M.Z., 1999. Contribution of vegetation to the water cycle of the Amazon basin: an
541 isotopic study of plant transpiration and its water source. University of Miami.
- 542 Negrón-Juárez, R. et al., 2020. Calibration, measurement, and characterization of soil moisture
543 dynamics in a central Amazonian tropical forest. *Vadose Zone Journal*, 19(1): e20070.
- 544 Nepstad, D. et al., 2002. The effects of partial throughfall exclusion on canopy processes,
545 aboveground production, and biogeochemistry of an Amazon forest. *Journal of*
546 *Geophysical Research: Atmospheres*, 107(D20): LBA 53-1-LBA 53-18.
- 547 Nepstad, D.C. et al., 1994. The role of deep roots in the hydrological and carbon cycles of
548 Amazonian forests and pastures. *Nature*, 372(6507): 666-669.
- 549 Nepstad, D.C., Tohver, I.M., Ray, D., Moutinho, P. and Cardinot, G., 2007. Mortality of large
550 trees and lianas following experimental drought in an Amazon forest. *Ecology*, 88(9):
551 2259-2269.
- 552 Nobre, C.A., Sellers, P.J. and Shukla, J., 1991. Amazonian deforestation and regional climate
553 change. *Journal of climate*, 4(10): 957-988.

- 554 Ohta, S., Ferraz, J.B.S. and Sales, P.C.d., 1998. Distribuição dos Solos Ao Longo de Dois
555 Transectos Em Floresta Primária Ao Norte de Manaus (Am). Pesquisas Florestais para a
556 Conservação da Floresta e Reabilitação de áreas Degradadas da Amazônia, pgs. 109-143.
- 557 Oliveira, R.S. et al., 2019. Embolism resistance drives the distribution of Amazonian rainforest
558 tree species along hydro-topographic gradients. *New Phytologist*, 221(3): 1457-1465.
- 559 Oliveira, R.S., Dawson, T.E., Burgess, S.S. and Nepstad, D.C., 2005. Hydraulic redistribution in
560 three Amazonian trees. *Oecologia*, 145(3): 354-363.
- 561 Oliveira, Rafael S., et al. 2021. Linking plant hydraulics and the fast–slow continuum to
562 understand resilience to drought in tropical ecosystems. *New Phytologist* 230.3: 904-923.
- 563 Parsons, L., 2020. Implications of CMIP6 projected drying trends for 21st century Amazonian
564 drought risk. *Earth's Future*, 8(10): e2020EF001608.
- 565 Powell, T.L. et al., 2013. Confronting model predictions of carbon fluxes with measurements of
566 Amazon forests subjected to experimental drought. *New Phytologist*, 200(2): 350-365.
- 567 Restrepo-Coupe, N. et al., 2013. What drives the seasonality of photosynthesis across the
568 Amazon basin? A cross-site analysis of eddy flux tower measurements from the Brasil
569 flux network. *Agricultural and Forest Meteorology*, 182: 128-144.
- 570 Roberts, J. et al., 1993. Transpiration from an Amazonian rainforest calculated from stomatal
571 conductance measurements. *Agricultural and Forest Meteorology*, 65(3-4): 175-196.
- 572 Saleska, S.R. et al., 2003. Carbon in Amazon forests: unexpected seasonal fluxes and
573 disturbance-induced losses. *Science*, 302(5650): 1554-1557.
- 574 Santos, V.A.H.F.d. et al., 2018. Causes of reduced leaf-level photosynthesis during strong El
575 Niño drought in a Central Amazon forest. *Global change biology*, 24(9): 4266-4279.
- 576 Shuttleworth, W.J., 1988. Evaporation from Amazonian rainforest. *Proceedings of the Royal
577 society of London. Series B. Biological sciences*, 233(1272): 321-346.
- 578 Smith, M.N. et al., 2019. Seasonal and drought-related changes in leaf area profiles depend on
579 height and light environment in an Amazon forest. *New Phytologist*, 222(3): 1284-1297.
- 580 Steppe, K., De Pauw, D.J., Doody, T.M. and Teskey, R.O., 2010. A comparison of sap flux
581 density using thermal dissipation, heat pulse velocity and heat field deformation methods.
582 *Agricultural and Forest Meteorology*, 150(7-8): 1046-1056.
- 583 Swann, Abigail LS, et al. 2016. Plant responses to increasing CO₂ reduce estimates of climate
584 impacts on drought severity. *Proceedings of the National Academy of Sciences* 113.36:
585 10019-10024.
- 586 Tang, H. and Dubayah, R., 2017. Light-driven growth in Amazon evergreen forests explained by
587 seasonal variations of vertical canopy structure. *Proceedings of the National Academy of
588 Sciences*, 114(10): 2640-2644.

- 589 Teixeira, W.G., Schroth, G., Marques, J.D. and Huwe, B., 2014. Unsaturated soil hydraulic
590 conductivity in the central Amazon: Field evaluations, *Application of Soil Physics in*
591 *Environmental Analyses*. Springer, pp. 283-305.
- 592 Van Genuchten, M.T., 1980. A closed-form equation for predicting the hydraulic conductivity of
593 unsaturated soils. *Soil science society of America journal*, 44(5): 892-898.
- 594 Vieira, S. et al., 2004. Forest structure and carbon dynamics in Amazonian tropical rain forests.
595 *Oecologia*, 140(3): 468-479.
- 596 Vogel, M.M., Hauser, M. and Seneviratne, S.I., 2020. Projected changes in hot, dry and wet
597 extreme events' clusters in CMIP6 multi-model ensemble. *Environmental Research*
598 *Letters*, 15(9): 094021.
- 599 Von Randow, C. et al., 2004. Comparative measurements and seasonal variations in energy and
600 carbon exchange over forest and pasture in South West Amazonia. *Theoretical and*
601 *Applied Climatology*, 78(1): 5-26.
- 602 Vourlitis, G.L. et al., 2002. Seasonal variations in the evapotranspiration of a transitional tropical
603 forest of Mato Grosso, Brazil. *Water resources research*, 38(6): 30-1-30-11.
- 604 Wright, J.S. et al., 2017. Rainforest-initiated wet season onset over the southern Amazon.
605 *Proceedings of the National Academy of Sciences*, 114(32): 8481-8486.
- 606 Wu, J. et al., 2016. Leaf development and demography explain photosynthetic seasonality in
607 Amazon evergreen forests. *Science*, 351(6276): 972-976.
- 608 Wu, J. et al., 2017. Partitioning controls on Amazon forest photosynthesis between
609 environmental and biotic factors at hourly to interannual timescales. *Global Change*
610 *Biology*, 23(3): 1240-1257.
- 611 Yang, J. et al., 2018. Amazon drought and forest response: Largely reduced forest photosynthesis
612 but slightly increased canopy greenness during the extreme drought of 2015/2016. *Global*
613 *change biology*, 24(5): 1919-1934.